arXiv:1510.08072v2 [hep-ph] 29 Oct 2015

Finite Numbers of Sources, Particle Correlations and the Color Glass Condensate

Larry McLerran[a,c], Vladimir V. Skokov[b]

[a] *Department of Physics, Brookhaven National Laboratory, Upton, NY 11973*
[b] *RIKEN/BNL, Brookhaven National Laboratory, Upton, NY 11973*
[c] *Physics Dept, China Central Normal University, Wuhan, China*

Abstract

We show that for a finite number of emitting sources, the Color Glass Condensate produces substantial elliptic azimuthal anisotropy, characterized by v_2, for two and four particle correlations for momentum greater than or of the order the saturation momentum. The flow produced has the correct semi-quantitative features to describe flow seen in LHC experiments with p-Pb and pp collisions. This flow is induced by quantum mechanical interference between the waves of produced particles, and the flow itself is coupled to fluctuations in the positions of emitting sources. We shortly discuss generalizing these results to odd v_n, to correlations involving larger number of particles, and to transverse momentum scales $\Lambda_{\rm QCD} \ll p_T \ll Q_{\rm sat}$.

1. Introduction

It has been shown in the LHC experiments that in both pA and pp collisions, there is a substantial azimuthal anisotropy, quantified by the second Fourier harmonics also often referred to as elliptic "flow", [1, 2, 3, 4, 5, 6, 7]. This anisotropy appears in the elliptic flow coefficient v_2 for two particle correlations in $v_2\{2\}$, and for pA collisions in four particle correlations $v_2\{4\}$ and for higher numbers of particles $v_2\{n\}$. There is also evidence for non-zero odd harmonics of the azimuthal anisotropy, v_3. These results suggest that a hydrodynamic treatment may be valid [8] in spite of the difficulty justifying such a description for such small systems [9]. It is nevertheless challenging to reconcile

with the observation that there is little evidence for jet quenching of particles at the same transverse momentum where particles flow [2], and the fact that flow is seen at high transverse momenta where hydrodynamic descriptions are questionable.

The coefficient v_2 for two particle correlations has on the other hand been computed within the theory of the Color Glass Condensate [10, 11, 12, 13, 14, 15], which for the lack of better terminology we will refer to as Glasma Graph (GG). This computation assumes a continuum of sources, and is in the limit of an infinite number of sources. The result is of order $1/N_c^2$ where N_c is the number of colors. As was later elucidated this suppression is a manifestation of Bose-Einstein enhancement of gluons in the target [16], see also discussions in Ref. [18, 17]. However, it has proven difficult to use GG mechanism to extract the four particle correlation $v_2\{4\}$ since computations almost invariably lead to a four particle correlation that is positive corresponding to an complex $v_2\{4\}$, see Refs. [19, 20, 21].

One can question the CGC treatment to date as it uses a continuum of emission sources. In pA, pp and peripheral AA collisions, there is good evidence that the ellipticity that might drive hydrodynamic flow is generated by fluctuations in the emission from a finite number of sources [22, 23, 24]. Ellipticities have been calculated that semi-quantitatively agree with extraction from hydrodynamic models of experiment.

In the systems driven by fluctuations, the ellipticities that fluctuations induce vanish in the limit of an infinite number of sources. In this limit the distribution becomes uniform. Therefore the GG CGC computations will always dominate over a fluctuation induced component for sufficiently high multiplicity in the momentum domain of GG CGC applicability. Nevertheless for the multiplicities experimentally accessible, one might not be in the asymptotic limit.

The corresponding computation of the emission from the CGC for a finite number of sources is the subject of this paper. We will find that there are two effects needed to generate an acceptable $v_2\{2\}$. The first is the finite number of sources. We also find that

we need to have a finite range color correlation length. This correlation length has been computed in the literature and shown to be of the order of the saturation momentum scale [25]. It arises in the evolution of gluon distribution functions. In the McLerran-Venugopalan model [26], the length is infinite, and one does not in this way generate an acceptable v_2.

Because the correlation length is of order $Q_{\rm sat}$, we will find that the characteristic momentum scale size associated with flow is the saturation momentum. Again, this is a surprise since one would have naively thought that wave interference of the emitting gluons would be on a characteristic momentum scale of the inverse source size, that is $1/R_{\rm nucleon}$ [27].

The purpose of this paper is to outline methods for the computation of $v_2\{n\}$. We explicitly compute $v_2\{2\}$, $v_4\{2\}$ and $v_2\{4\}$. We restrict our computations to transverse momentum scales greater than or of the order of that of the nuclear saturation momentum. There is no difficulty in principle computing in the extended range where $\Lambda_{\rm QCD} \ll p_\perp \ll Q_{\rm sat}$, but as a first attempt to demonstrate the method we restrict the range of momentum.

We find a semi-quantitative agreement with the experimentally measured $v_2\{2\}$. The magnitude and dependence upon $p_\perp$ appear to be roughly in agreement with experiment for reasonable choices of our parameter. We also will show that the result factorizes for momentum scales consistent with out approximation and in accord with experimental results. It is more complicated for us to compute $v_2\{n\}$ for $n \geq 4$. We can do this as an expansion in the inverse of the number of particles sources, and have done so for $v_2\{4\}$, and achieve an acceptable result. The computation of $v_2\{6\}$ and higher is complicated and we do not explicitly compute here, although we point out the complications of such a computation.

We believe that computing a non-vanishing v_3 should be possible using the techniques we outline here. This involves a three gluon odderon type emission, which should generate odd two particle correlations. This is an interesting quantity to compute, and we hope to

return to this in a later paper.

We note that present classical Yang-Mills simulations already indicate the presence of v_3, it develops due to time evolution and non-linearity of the Yang-Mills equations of motion, see Ref. [28].

We caution the reader that the rough agreement we find with experimentally determined flow values is probably accidental and arises from adjusting parameters, since we expect the GG $1/N_c^2$ correction to contribute for high multiplicity events, and that final state interactions of particles need to be taken into account either through hydrodynamics or transport computations. Our computation should be viewed as complementing the results from the Glasma on initial conditions, and are amusing since these results the initial conditions have a good deal of collectivity, in the form of initial state flow. Our computation supplements the results on initial state fluctuation driven ellipticity, and generate flow in the initial state since quantum mechanics forces non-trivial interference between the wavefunctions of particle produced from discrete sources which appear in the momentum space amplitudes. We also caution the reader that we are outlining here the beginnings of more detailed computations which allow one to extend results to wider range of momenta, correlations with larger number of particles, and hopefully for v_3.

2. Color Correlations

We begin with a discussion of the finite correlation length for color charge in the Color Glass Condensate. It was shown that upon evolution, there is a finite color neutralization length in the CGC [25]. The specific form of the propagator was shown to have an anomalous dimension, and a range of order the inverse saturation momentum scale. In the treatment we present here, we will include the finite range of color charge correlations but we will not include the effects of anomalous dimension. The inclusion of an anomalous dimension presents no problem in principle but obscures the qualitative and semi-quantitative points we wish to make.

We assume that in the continuum

$$\langle \rho^a(\vec{k})\rho^b(\vec{q})\rangle = (2\pi)^2\delta^{ab}\delta(\vec{k}+\vec{q})\Delta(\vec{k}), \tag{1}$$

where we approximate

$$\Delta(\vec{k}) = \frac{\mu^2 k^2}{k^2+m^2}. \tag{2}$$

Here $m = \kappa Q_s$ and κ is a free parameter of order one. Equation Eq. (2) is the simplest analytic generalization of the McLerran-Venugopalan model which takes into account the color neutralization phenomena discussed in details in Ref. [25]. It also in agreement with the double-logarithmic approximation of BFKL at a very high transverse momentum.

For future purpose we want to express μ^2 in terms of the number of sources. Lets consider the MV model

$$\langle \rho^a(\vec{x})\rho^b(\vec{y})\rangle = \delta^{ab}\delta(\vec{x}-\vec{y})\mu^2 \tag{3}$$

to compute

$$\langle Q^a Q^a\rangle = d_A \int d^2x d^2y \delta(\vec{x}-\vec{y})\mu^2 = d_A S_\perp \mu^2, \tag{4}$$

where $Q^a = \int d^2x \rho^a(\vec{x})$ and $d_A = N_c^2 - 1$ is the dimension of the adjoint representation. From the other hand

$$\langle Q^a Q^a\rangle = \mathrm{tr}\left(g^2 T_R^a T_R^a N\right) = g^2 C_R d_R N, \tag{5}$$

where $C_R(d_R)$ is the Casimir (dimension) of the representation R, for the adjoint (fundamental) representation $C_A = N_c$ ($C_F = (N_c^2-1)/2N_c$). Combining Eqs. (4) and (5), we obtain

$$S_\perp \mu^2 = \frac{g^2 C_R d_R}{d_A} N. \tag{6}$$

In coordinate space,

$$\Delta(\vec{x}) = \int \frac{d^2k}{(2\pi)^2}\Delta(k) e^{i\vec{k}\vec{x}}. \tag{7}$$

The propagator $\Delta(\vec{x})$ is the charge density correlation function, i.e.

$$\langle \rho^a(\vec{x})\rho^b(\vec{y})\rangle = \delta^{ab}\Delta(\vec{x}-\vec{y}). \tag{8}$$

Explicitly, computing the Fourier transformation of Eq. (7) we obtain

$$\Delta(\vec{x}) = \mu^2 \left[\delta(\vec{x}) - \frac{m^2}{2\pi} K_0(|\vec{x}|m) \right]. \tag{9}$$

Note that the presence of the factors of k^2 in the numerators of $\Delta(k)$ guarantees charge neutralization, since then

$$\int d^2x \ \Delta(x) = 0. \tag{10}$$

To define Q_s the scattering matrix is to be computed

$$S(r_\perp) = \exp\left(-g^2 C_R \int \frac{d^2k_\perp}{(2\pi)^2} \frac{\Delta(k)}{k^4} \left[1 - e^{i\vec{k}_\perp \vec{r}_\perp} \right] \right) = \tag{11}$$

$$\exp\left(-\frac{g^2}{2\pi} C_R \frac{\mu^2}{m^2} \left[\gamma_E + K_0(mr_\perp) + \ln\left(\frac{mr_\perp}{2} \right) \right] \right). \tag{12}$$

Conventionally Q_s is define in the limit $m \to 0$, where $S_\perp = \exp(-Q_s^2 r^2 \ln(1/\Lambda^2 r^2)/4)$ with

$$Q_s^2 = \alpha C_R \mu^2 \tag{13}$$

and $\Lambda = m e^{\gamma_E - 1}/2$. Equations (6) and (13) give us another useful relation

$$S_\perp Q_s^2 = 4\pi \frac{\alpha^2 C_R^2 d_R}{d_A} N. \tag{14}$$

Lets consider a target with sources at positions $\vec{x}_i$, $i = 1, \ldots, N$. We will assume the sources are randomly distributed within some circular region of area $S_\perp$, where the circular region corresponds to the that of the interaction region. Thus the color density of the target is given by

$$\rho^a(\vec{x}) = \sum_i \xi_i^a \delta(\vec{x} - \vec{x}_i). \tag{15}$$

The Fourier transform of the distribution is given by

$$\rho^a(\vec{k}) = \int d^2x e^{-i\vec{k}\vec{x}} \rho(\vec{x}) = \sum_i \xi_i^a e^{-i\vec{k}\vec{x}_i}. \tag{16}$$

To derive the correlator for ξ_i^a, lets consider

$$\langle \rho^a(y) \rho^b(z) \rangle = \int \frac{d^2x_1}{S_\perp} \cdots \frac{d^2x_N}{S_\perp} \sum_{i,j} \langle \xi(x_i)^a \xi(x_j)^b \rangle \delta(y - x_i) \delta(z - x_j) =$$

$$\delta^{ab} \frac{N(N-1)}{S_\perp^2} \chi(z - y) + \delta^{ab} \frac{N}{S_\perp} \delta(z - y) \chi_0, \tag{17}$$

where

$$\langle \xi^a(x)\xi^b(y)\rangle = \delta^{ab}\chi(x-y) \tag{18}$$

and

$$\langle \xi^a(x)\xi^b(x)\rangle = \delta^{ab}\chi_0. \tag{19}$$

From Eqs. (9) and (19) we find

$$\chi_0 = \frac{\sigma}{N}, \tag{20}$$

where we introduced the dimensionless transverse area with the physical meaning of the average charge squared per degree of freedom,

$$\sigma = \mu^2 S_\perp. \tag{21}$$

The nontrivial dependence of the correlator on position is obtained from matching terms of Eq. (9) and (17)

$$\chi(x) = -\frac{\sigma^2}{2\pi N(N-1)}\left(\frac{m}{\mu}\right)^2 K_0(|\vec{x}|m). \tag{22}$$

The Fourier transform of the latter is

$$\chi(k) = -\frac{\sigma^2}{N(N-1)}\left(\frac{m}{\mu}\right)^2 \frac{1}{k^2+m^2}. \tag{23}$$

3. S-matrix

In this section we consider one, two and four-particle inclusive S-matrix. The results will be used in the next section to calculated the harmonics of the azimuthal anisotropy.

3.1. Single particle scattering

For fixed positions of the sources, the S-matrix describing scattering of a quark off the target for a fixed configuration of the latter is

$$S(\vec{y}_1,\vec{y}_2) = \frac{1}{N_c}\mathrm{tr}\left(V^\dagger(\vec{y}_1)V(\vec{y}_2)\right) \tag{24}$$

and in the dilute limit it simplifies to

$$S-1 = -\frac{g^2}{4N_c}\left(\alpha^a(\vec{y}_1)-\alpha^a(\vec{y}_2)\right)^2, \tag{25}$$

where

$$-\nabla^2\alpha^a(\vec{x}) = \rho_a(\vec{x}) \tag{26}$$

and thus

$$\alpha^a(\vec{k}) = \sum_i \xi_i^a \frac{1}{k^2} e^{-i\vec{k}\vec{x}_i}. \tag{27}$$

Performing Fourier transformation we obtain

$$S(\vec{p},\vec{b}) - 1 = -\frac{g^2}{N_c}\int \frac{d^2k}{(2\pi)^2}\left[\alpha^a(\vec{k}+\vec{p})\alpha^a(\vec{p}-\vec{k})e^{2i\vec{b}\vec{p}} + \text{c.c.} - 2\alpha^a(\vec{k}+\vec{p})\alpha^a(\vec{k}-\vec{p})e^{2i\vec{k}\vec{b}}\right]. \tag{28}$$

Integrating with respect to the impact parameter one gets

$$S(\vec{p},\vec{x}_1,\ldots,\vec{x}_N) - 1 = -\frac{g^2}{2N_c}\left(\delta(\vec{p})\int d^2k|\alpha^a(k)|^2 - |\alpha^a(\vec{p})|^2\right). \tag{29}$$

The first term is not of the interest to us; it is related to the inverse is of the projectile. Substituting Eq. (27) we get

$$S(\vec{p},\vec{x}_1,\ldots,\vec{x}_N) - 1 = \frac{g^2}{2N_c}\frac{1}{p^4}\sum_{i,j}\xi_i^a\xi_j^a e^{-i\vec{p}(\vec{x}_i-\vec{x}_j)} = \frac{g^2}{2N_c}\frac{1}{p^4}\left(\xi_i^a\xi_i^a + \sum_{i\neq j}\xi_i^a\xi_j^a e^{-i\vec{p}(\vec{x}_i-\vec{x}_j)}\right). \tag{30}$$

The experimentally measured one particle inclusive S-matrix can be obtained by averaging Eq. (30) with respect to all possible sources' positions and configurations of ξ_i^a.

3.2. Two particle scattering

To extract the two-particle azimuthal anisotropy, the two particle S-matrix is to be computed

$$\langle S_2(\vec{p}_1,\vec{p}_2)\rangle = S_\perp^{-N}\int\left(\Pi_l d^2x_l\right)\langle S(\vec{p}_1,\vec{x}_1,\ldots,\vec{x}_N)S(\vec{p}_2,\vec{x}_1,\ldots,\vec{x}_N)\rangle =$$

$$S_\perp^{-N}\int\left(\Pi_l d^2x_l\right)\sum_{i,j}\sum_{i',j'}\left(\frac{g^2}{2N_c}\right)^2\frac{1}{p_1^4p_2^4}\left\langle\sum_{i,j}\xi_i^a\xi_j^a e^{-i\vec{p}_1(\vec{x}_i-\vec{x}_j)}\sum_{i',j'}\xi_{i'}^b\xi_{j'}^b e^{-i\vec{p}_2(\vec{x}_{i'}-\vec{x}_{j'})}\right\rangle \underset{=}{\text{Large } N_c}$$

$$\left(\frac{g^2}{2N_c}\right)^2\frac{(N_c^2-1)^2}{p_1^4p_2^4}\frac{1}{S_\perp^2}\left(\chi(p_1)\chi(p_2)\left[\frac{N!}{(N-4)!}+4\frac{N!}{(N-3)!}\right]+\frac{NN!S_\perp}{(N-2)!}\chi_0\left[\chi(p_1)+\chi(p_2)\right]+\right.$$

$$\left.S_\perp^2N^2\chi_0^2+\frac{S_\perp N!}{(N-2)!}\left[\chi_2(p_1+p_2)+\chi_2(p_1-p_2)\right]\right), \tag{31}$$

where

$$\chi_2(p) = \int d^2x e^{ipx}\chi^2(x) = \frac{2\pi}{m^2}\left[\frac{\sigma^2}{2\pi N(N-1)}\left(\frac{m}{\mu}\right)^2\right]^2 I(p), \quad I(p) = \frac{m\,\sinh^{-1}\left(\frac{p}{2m}\right)}{p\sqrt{1+\left(\frac{p}{2m}\right)^2}}. \tag{32}$$

For small (large) p, $I(p \ll m) \approx \frac{1}{2}\left(1 - \frac{p^2}{6m^2}\right)$ ($I(p \gg m) \approx \frac{m^2}{p^2}\ln\left(\frac{p^2}{m^2}\right)$). The second equality in Eq. (31) is only valid in the large N_c limit because the connected contributions (in term of the color indices), also called the "glasma" graphs were neglected. They are however important to be accounted for in the limit of infinite number of sources, as we discussed in the Introduction.

The azimuthal anisotropy can arise only from the last term of Eq. (31). The Fourier components of $\chi_2(p_1+p_2)$ for an even n are given by

$$\langle\chi_2(p_1+p_2)e^{in(\phi_1-\phi_2)}\rangle \equiv \int \frac{d\phi_1}{2\pi}\frac{d\phi_2}{2\pi}\chi_2(p_1+p_2) = \int d^2x J_n(|p_1||x|)J_n(|p_2||x|)\chi^2(x) = 2\pi\int dx x J_n(|p_1||x|)J_n(|p_2||x|)\chi^2(x). \tag{33}$$

An analytic expression for the Fourier components can be derived if $|p_1| = |p_2| = p$

$$\langle\chi_2(p_1+p_2)e^{in(\phi_1-\phi_2)}\rangle_{|p_1|=|p_2|=p} = \frac{2\pi}{m^2}\left[\frac{\sigma^2}{2\pi N(N-1)}\left(\frac{m}{\mu}\right)^2\right]^2 I_n(p). \tag{34}$$

For the relevant values of n we get

$$I_0(p) = \frac{m}{2p}\tan^{-1}\left(\frac{p}{m}\right) \tag{35}$$

and

$$I_2(p) = I_0(p) + \frac{m^2}{p^2}\left[1 - \left(1+\frac{m^2}{p^2}\right)\ln\left(1+\frac{p^2}{m^2}\right)\right]. \tag{36}$$

In the next section the numerical computations of Eq. (31) will be performed, here we only want to discuss the general structure of the S-matrix. To simplify matters for now,

let us consider the large N limit of Eq. (31):

$$\langle S_2(\vec{p}_1,\vec{p}_2)\rangle_{\text{Large } N} = \left(\frac{g^2}{2N_c}\right)^2 \frac{(N_c^2-1)^2}{p_1^4 p_2^4}\sigma^2 \left[\frac{1}{(p_1^2+m^2)(p_2^2+m^2)}\left(p_1^2p_2^2 - \frac{2m^4}{N^2}\right) + \frac{\sigma}{2\pi N^2}\left(\frac{m}{\mu}\right)^2 (I(\vec{p}_1+\vec{p}_2)+I(\vec{p}_1-\vec{p}_2))\right]. \quad (37)$$

As can be seen from Eq. (37) the azimuthally anisotropic part is proportional to $\frac{\sigma}{N^2}\left(\frac{m}{\mu}\right)^2$. Previously we established that $\sigma \propto N$ and thus the amplitude of the azimuthal anisotropy is suppressed by N^{-1} instead of a naive N^{-2}. The remaining factor of $\left(\frac{m}{\mu}\right)^2 = \alpha C_R \kappa^2$. Thus the amplitude is also controlled by the free parameter κ. The factor of αC_R is of order one in the relevant energy range.

3.3. Four particle scattering

Due to its phenomenological importance we also compute four-particle S-matrix. We were able to do this only in the limit $|p_1| = |p_2| = |p_3| = |p_4| = p$ and we neglected the contributions suppressed by powers of N when they are not compensated by large combinatorics factors. The full calculations of the four-particle S-matrix become very involved and will not make any significant difference for the numerical results presented

in the next section. Straightforward computations yield

$$\langle S_4(\vec{p}_1,\vec{p}_2,\vec{p}_3,\vec{p}_4)\rangle = \left(\frac{g^2}{2N_c}\right)^4 \left(\frac{N_c^2-1}{p^4}\right)^4$$
$$\left\{\frac{\chi^4(p)}{S_\perp^4}\left[\frac{N!}{(N-8)!}+2^2\binom{2}{4}\frac{N!}{(N-7)!}+2^4\binom{2}{4}\frac{N!}{(N-6)!}+2^3\binom{1}{4}\binom{1}{3}\frac{N!}{(N-6)!}+2^5\binom{2}{4}\frac{N!}{(N-5)!}\right]+\right.$$
$$\frac{\chi^3(p)}{S_\perp^3}\binom{1}{4}N\chi_0\left[\frac{N!}{(N-6)!}+2^2\binom{1}{3}\frac{N!}{(N-5)!}+2^3\binom{1}{3}\frac{N!}{(N-4)!}\right]+$$
$$\chi_0^2\frac{\chi^2(p)}{S_\perp^2}\binom{2}{4}N^2\left[\frac{N!}{(N-4)!}+2^2\frac{N!}{(N-3)!}\right]+\chi_0^3\frac{\chi(p)}{S_\perp}\binom{1}{4}N^3\frac{N!}{(N-2)!}+N^4\chi_0^4+$$
$$\frac{N!}{(N-4)!}\left[\left(\frac{\chi_2(p_1+p_2)}{S_\perp}+\frac{\chi_2(p_1-p_2)}{S_\perp}\right)\left(\frac{\chi_2(p_3+p_4)}{S_\perp}+\frac{\chi_2(p_3-p_4)}{S_\perp}\right)+\right.$$
$$\left(\frac{\chi_2(p_1+p_3)}{S_\perp}+\frac{\chi_2(p_1-p_3)}{S_\perp}\right)\left(\frac{\chi_2(p_2+p_4)}{S_\perp}+\frac{\chi_2(p_2-p_4)}{S_\perp}\right)+$$
$$\left.\left(\frac{\chi_2(p_1+p_4)}{S_\perp}+\frac{\chi_2(p_1-p_4)}{S_\perp}\right)\left(\frac{\chi_2(p_2+p_3)}{S_\perp}+\frac{\chi_2(p_2-p_3)}{S_\perp}\right)\right]+$$
$$\left.\frac{N!}{(N-2)}\left[\frac{\chi_4(p_1+p_2+p_3+p_4)}{S_\perp}+\quad\text{sign permutations in front of } p_{2,3,4}\right]\right\} = \left(\frac{g^2}{2N_c}\right)^4\left(\frac{N_c^2-1}{p^4}\right)^4$$
$$\left\{\frac{\chi^4(p)}{S_\perp^4}\left[\frac{N!}{(N-5)!}(N^3+6N^2+35N-258)\right]+\right.$$
$$\frac{\chi^3(p)}{S_\perp^3}4N\chi_0\left[\frac{N!}{(N-4)!}(N-1)(N+4)\right]+$$
$$\chi_0^2\frac{\chi^2(p)}{S_\perp^2}6N^2\left[\frac{N!}{(N-3)!}(N+1)\right]+\chi_0^3\frac{\chi(p)}{S_\perp}4N^4(N-1)+N^4\chi_0^4+$$
$$\frac{N!}{(N-4)!}\left[\left(\frac{\chi_2(p_1+p_2)}{S_\perp}+\frac{\chi_2(p_1-p_2)}{S_\perp}\right)\left(\frac{\chi_2(p_3+p_4)}{S_\perp}+\frac{\chi_2(p_3-p_4)}{S_\perp}\right)+\right.$$
$$\left(\frac{\chi_2(p_1+p_3)}{S_\perp}+\frac{\chi_2(p_1-p_3)}{S_\perp}\right)\left(\frac{\chi_2(p_2+p_4)}{S_\perp}+\frac{\chi_2(p_2-p_4)}{S_\perp}\right)+$$
$$\left.\left.\left(\frac{\chi_2(p_1+p_4)}{S_\perp}+\frac{\chi_2(p_1-p_4)}{S_\perp}\right)\left(\frac{\chi_2(p_2+p_3)}{S_\perp}+\frac{\chi_2(p_2-p_3)}{S_\perp}\right)\right]\right\}+$$
$$\left.\frac{N!}{(N-2)}\left[\frac{\chi_4(p_1+p_2+p_3+p_4)}{S_\perp}+\quad\text{sign permutations in front of } p_{2,3,4}\right]\right. . \quad (38)$$

Here we introduced

$$\chi_4(p) = \int d^2x e^{ixp}\chi^4(x). \quad (39)$$

For the numerical calculations presented in the next section we need only the following angular average

$$\langle \chi_4(p_1 \pm p_2 \pm p_3 \pm p_4) e^{in(\phi_1+\phi_2-\phi_3-\phi_4)} \rangle_{|p_i|=p} = \frac{2\pi}{m^2} \left[\frac{\sigma^2}{2\pi N(N-1)} \left(\frac{m}{\mu} \right)^2 \right]^4 Y_n(p), \quad Y_n(p) = \int_0^\infty dx x J_n^4 \left(\frac{p}{m} x \right) K_0^4(x). \quad (40)$$

4. Harmonics of azimuthal anisotropy

Using the results of the previous section we will extract the harmonics of the azimuthal anisotropy. The derivation was performed for the fundamental representation of the Wilson lines, but in the dilute limit, we operate in, the Casimirs and the dimension of representations enter as overall numerical constants. Thus the results in the adjoint representation for the observables we are about to consider will be the same as for the fundamental.

For two-particle azimuthal anisotropy, we follow the definitions commonly accepted in the community. The two-particle azimuthal anisotropy is given by

$$v_2\{n\}(p_\perp) = \frac{V_{n\Delta}(p_\perp, p_\perp^{\rm Ref})}{\sqrt{V_{n\Delta}(p_\perp^{\rm Ref}, p_\perp^{\rm Ref})}}, \quad (41)$$

where

$$V_{n\Delta}(p_\perp^{\rm A}, p_\perp^{\rm B}) = \frac{\langle S_2(p_\perp^{\rm A}, p_\perp^{\rm B}) \exp\left(in\Delta\phi\right) \rangle}{\langle S_2(p_\perp^{\rm A}, p_\perp^{\rm B}) \rangle}. \quad (42)$$

In our model we have a few free parameters, Q_s, κ and N. The number of sources can be in principal fixed by performing Monte-Carlo simulations and triggering number of produced particles. This however will require an access to the soft momentum range, where the dilute approximation breaks down and our model cannot be formally applied. Thus we keep the number of sources to be a free parameter ranging from 10 to 25. The results of the fit of the experimental data results in $N = 15$. Again we present this result with a grain of salt: given the approximations we made they are at best qualitative and cannot be considered as a quantitative outcome of the model. Nonetheless we think it is

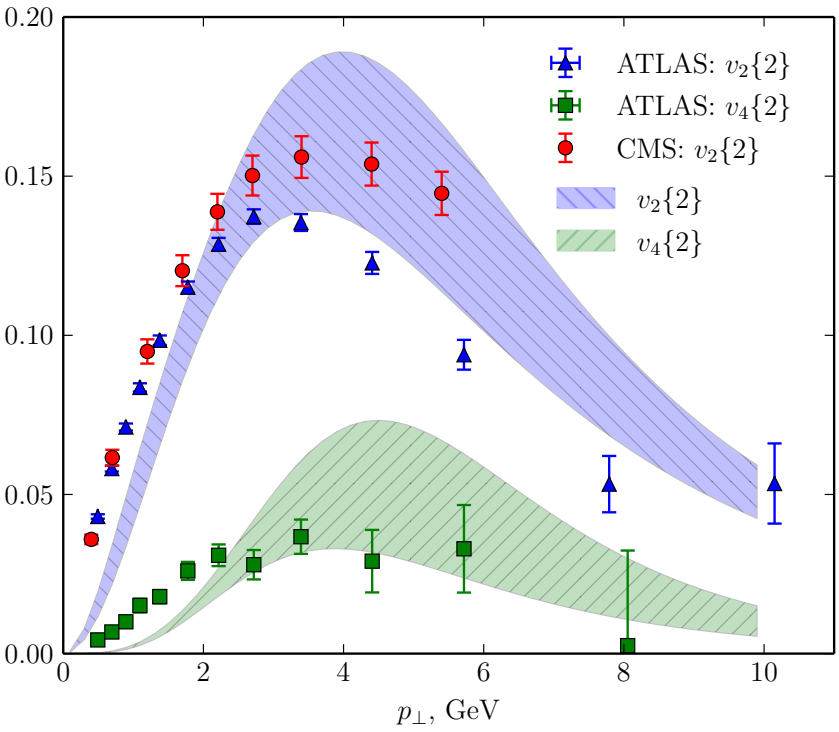

Figure 1: The azimuthal anisotropy harmonics $v_2\{2\}$ and $v_4\{2\}$ as a function of the transverse momentum. The bands correspond to the model results with $p_\perp^{\rm Ref}$ varying from 1 to 3 GeV. The ATLAS data is for 1 GeV $< p_\perp <$ 3 GeV and $220 < N_{\rm ch} < 260$, see Ref. [5]. The CMS data is for 0.3 GeV $< p_\perp <$ 3 GeV and $220 < N_{\rm ch} < 260$, see Ref. [3]. The model parameters are $Q_s = 1.2$ GeV, $\kappa = 1.7$ and $N = 15$.

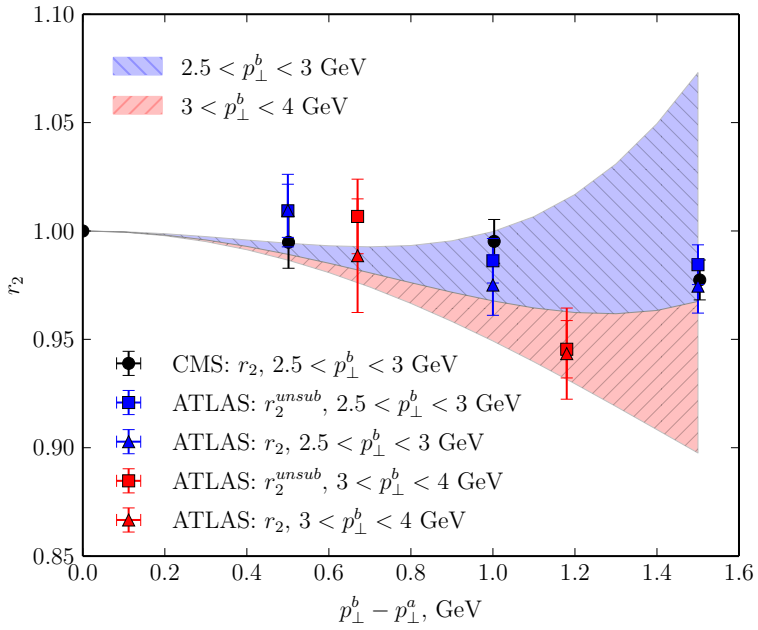

Figure 2: The ratio r_2 at a function of the momentum difference. The ATLAS and CMS data are from Refs. [5, 29] respectively. The experimental data are for $220 < N_{\rm ch} < 260$. The model parameters are the same as in Fig. 1.

important to demonstrate the model ability to fit the experimental data with a reasonable parameter set. The results for this fit are presented in Fig. 1. We used Q_s, κ and N to fit $v_2\{2\}$; $v_4\{2\}$ is the "prediction" of the model.

Lets also discuss another important observable which probes decorrelation of the harmonics in the transverse momentum. It is defined by

$$r_n = \frac{V_{N\Delta}(p_\perp^{\rm A}, p_\perp^{\rm B})}{\sqrt{V_{N\Delta}(p_\perp^{\rm A}, p_\perp^{\rm A}) V_{N\Delta}(p_\perp^{\rm B}, p_\perp^{\rm B})}}. \tag{43}$$

In the model the decorrelation is governed by m^2 and thus is close to one and does not depend on momentum at very high momenta. In the range of the model applicability we obtained the results shown in the Fig. 2. The description of the data is satisfactory.

Since we were not able to compute the four-particle correlation function for arbitrary momenta, the direct comparison with the experimental data for $v_2\{4\}$ is not possible. Nevertheless, to qualitatively examine the four-particle azimuthal anisotropy we compute

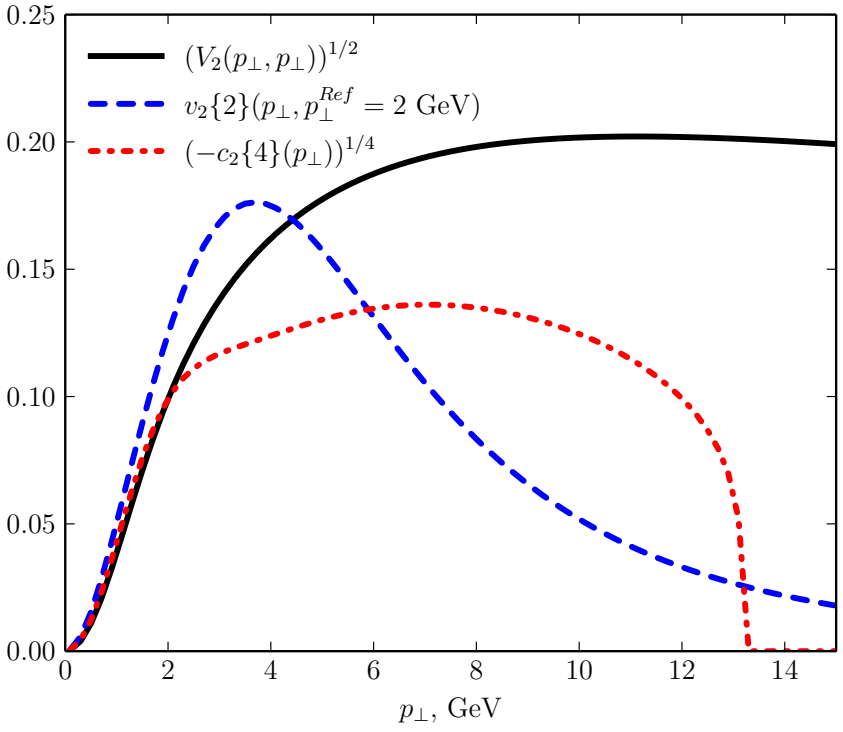

Figure 3: Comparison of the second Fourier harmonics computed from two-particle correlation function at the same momentum $(V_{2\Delta})^{1/2}$ and using the definition (41).

$c_2\{4\}(p_\perp)$ when all particles are taken at the same momenta. The result for $N = 10$, $Q_s = 1.2$ GeV and $\kappa = 1.7$ is presented in Fig. 3.

We compare $(-c_2\{4\}(p_\perp))^{1/4}$ to $v_2\{2\}$ and $(V_{n\Delta}(p_\perp, p_\perp))^{1/2}$. First of all there is a very striking difference between two different ways to compute the two-particle azimuthal anisotropy: the $v_2\{2\}$, computed according to the experimental prescription Eq. (41), decays fast with the momentum, while $(V_{n\Delta}(p_\perp, p_\perp))^{1/2}$ show almost no dependence on the momentum at high $p_\perp$. Second, the four particle azimuthal anisotropy defined by $(-c_2\{4\}(p_\perp))^{1/4}$ is very close to the one defined by two particles. Moreover $c_2\{4\}(p_\perp))$ is negative in the range of momentum relevant to the phenomenology and changes sign at about 13.5 GeV. Note that this numerical value may change once the connected contributions of GG or other local in rapidity background effects are taken into account, which presumable will lower this number.

5. Conclusions

In this paper we performed first computations of the azimuthal anisotropy in CGC with finite number of sources for momentum of particles greater than or of the order of the saturation momentum. This computation should be viewed as the precursor to refinements which allow computation for $\Lambda_{QCD} \ll p_T \ll Q_{sat}$, and for higher order particle cumulants such as $v_2\{n\}$ for $n \geq 6$. We also need to find a way to compute an initial $v_3\{2\}$.

This computation should be viewed in a larger framework: What are the initial values of ellipticities and flow moment predicted by first principles in QCD? Then another question is how are these initial values modified by final state interactions, be they hydrodynamic or transport generated. Without proper first principle computation of both final state and initial state physics, the beautiful experimental results showing flow in the high multiplicity collisions of small systems cannot be properly understood.

6. Acknowledgements

The authors gratefully acknowledge the comments of Jean Paul Blaizot, Soren Schlichting, Bjoern Schenke, Raju Venugopalan and Ulrich Heinz.

Larry McLerran is supported under Department of Energy contract number Contract No. DE-SC0012704.

References

[1] V. Khachatryan *et al.* [CMS Collaboration], JHEP **1009**, 091 (2010) [arXiv:1009.4122 [hep-ex]].

[2] S. Chatrchyan *et al.* [CMS Collaboration], Phys. Lett. B **718**, 795 (2013) [arXiv:1210.5482 [nucl-ex]].

[3] S. Chatrchyan *et al.* [CMS Collaboration], Phys. Lett. B **724**, 213 (2013) [arXiv:1305.0609 [nucl-ex]].

[4] G. Aad *et al.* [ATLAS Collaboration], Phys. Rev. Lett. **110**, no. 18, 182302 (2013) [arXiv:1212.5198 [hep-ex]].

[5] G. Aad *et al.* [ATLAS Collaboration], Phys. Rev. C **90**, no. 4, 044906 (2014) [arXiv:1409.1792 [hep-ex]].

[6] B. Abelev *et al.* [ALICE Collaboration], Phys. Lett. B **719**, 29 (2013) [arXiv:1212.2001 [nucl-ex]].

[7] B. B. Abelev *et al.* [ALICE Collaboration], Phys. Lett. B **726**, 164 (2013) [arXiv:1307.3237 [nucl-ex]].

[8] P. Bozek and W. Broniowski, Phys. Lett. B **718**, 1557 (2013) [arXiv:1211.0845 [nucl-th]].

[9] A. Bzdak, B. Schenke, P. Tribedy and R. Venugopalan, Phys. Rev. C **87**, no. 6, 064906 (2013) [arXiv:1304.3403 [nucl-th]].

[10] A. Dumitru, F. Gelis, L. McLerran and R. Venugopalan, Nucl. Phys. A **810**, 91 (2008) [arXiv:0804.3858 [hep-ph]].

[11] K. Dusling, F. Gelis, T. Lappi and R. Venugopalan, Nucl. Phys. A **836**, 159 (2010) [arXiv:0911.2720 [hep-ph]].

[12] A. Dumitru, K. Dusling, F. Gelis, J. Jalilian-Marian, T. Lappi and R. Venugopalan, Phys. Lett. B **697**, 21 (2011) [arXiv:1009.5295 [hep-ph]].

[13] E. Levin and A. H. Rezaeian, Phys. Rev. D **84**, 034031 (2011) [arXiv:1105.3275 [hep-ph]].

[14] K. Dusling and R. Venugopalan, Phys. Rev. D **87**, no. 5, 054014 (2013) [arXiv:1211.3701 [hep-ph]].

[15] Y. V. Kovchegov and D. E. Wertepny, Nucl. Phys. A **906**, 50 (2013) [arXiv:1212.1195 [hep-ph]].

[16] T. Altinoluk, N. Armesto, G. Beuf, A. Kovner and M. Lublinsky, arXiv:1503.07126 [hep-ph].

[17] A. Kovner and M. Lublinsky, Phys. Rev. D **84**, 094011 (2011) [arXiv:1109.0347 [hep-ph]].

[18] A. Kovner and M. Lublinsky, Int. J. Mod. Phys. E **22**, 1330001 (2013) [arXiv:1211.1928 [hep-ph]].

[19] A. Dumitru, L. McLerran and V. Skokov, Phys. Lett. B **743**, 134 (2015) [arXiv:1410.4844 [hep-ph]].

[20] V. Skokov, Phys. Rev. D **91**, no. 5, 054014 (2015) [arXiv:1412.5191 [hep-ph]].

[21] A. Dumitru, A. V. Giannini and V. Skokov, arXiv:1503.03897 [hep-ph].

[22] A. Bzdak, P. Bozek and L. McLerran, Nucl. Phys. A **927**, 15 (2014) [arXiv:1311.7325 [hep-ph]].

[23] L. Yan and J. Y. Ollitrault, Phys. Rev. Lett. **112**, 082301 (2014) [arXiv:1312.6555 [nucl-th]].

[24] A. Bzdak and V. Skokov, Nucl. Phys. A **943**, 1 (2015) [arXiv:1312.7349 [hep-ph]].

[25] E. Iancu, K. Itakura and L. McLerran, Nucl. Phys. A **724**, 181 (2003) [hep-ph/0212123].

[26] L. D. McLerran and R. Venugopalan, Phys. Rev. D **49** (1994) 2233 [hep-ph/9309289].

[27] D. Molnar, F. Wang and C. H. Greene, arXiv:1404.4119 [nucl-th].

[28] B. Schenke, S. Schlichting and R. Venugopalan, Phys. Lett. B **747**, 76 (2015) [arXiv:1502.01331 [hep-ph]].

[29] V. Khachatryan *et al.* [CMS Collaboration], Phys. Rev. C **92**, no. 3, 034911 (2015) [arXiv:1503.01692 [nucl-ex]].